

## Numerical and Experimental Investigation of Carbon Nanotube Sock Formation

Guangfeng Hou<sup>1</sup>, Vianessa Ng<sup>1</sup>, Yi Song<sup>1</sup>, Lu Zhang<sup>1</sup>, Chenhao Xu<sup>1</sup>, Vesselin Shanov<sup>1</sup>, David Mast<sup>2</sup>, Mark Schulz<sup>1\*</sup>, Yijun Liu<sup>1</sup>

<sup>1</sup> Department of Mechanical and Materials Engineering, University of Cincinnati, OH 45221, United States

<sup>2</sup> Department of Physics, University of Cincinnati, OH 45221, United States

### ABSTRACT

Formation of the carbon nanotube (CNT) sock, which is an assemblage of nanotubes in a thin cylindrical shape, is a prerequisite for continuous production of thread and sheet using the floating catalyst growth method. Although several studies have considered sock formation mechanisms, the dynamics of the sock behavior during the synthesis process are not well understood. In this work, a computational technique is utilized to explore the multiphysics environment within the nanotube reactor affecting the sock formation and structure. Specifically the flow field, temperature profile, catalyst nucleation, and residence time are investigated and their influence on the sock formation and properties are studied. We demonstrate that it is critical to control the multiphysics synthesis environment in order to form a stable sock. Sock production rate was studied experimentally and found to be linearly dependent on the amount of *effective* catalyst (iron in the sock) inside the reactor. To achieve a high sock production rate, the proportion of effective iron has to be high when increasing the total amount of catalyst in the reactor. Based on the analysis, we suggest that using small size catalyst and growing longer CNTs by increasing temperature, increasing residence times etc. will increase the CNT production rate and improve the properties of CNT thread/sheet produced from the sock.

### INTRODUCTION

Carbon nanotubes (CNTs) are a promising high-performance material due to their high mechanical, electrical and thermal properties. CNTs can be directly used in integrated circuits<sup>1</sup>, or processed into CNT thread or tape for various applications<sup>2,3</sup>. CNT thread can be produced by several methods: (i) dry spinning from a vertically aligned CNT array<sup>4</sup>, (ii) wet spinning from a CNT suspension<sup>5</sup>, and (iii) continuous direct-spinning from an aerogel-like sock in a floating catalyst type reactor<sup>6</sup>. Among these methods, the floating catalyst reactor is one of the most promising candidates for scaling up CNT production, due to high reaction rates and ease of making fibers and tapes. For CNT yarn, tape or sheet production by the floating catalyst method, a CNT sock is the prerequisite material where all the tubes within a sock are bonded through the CNT  $\pi$  bond interactions and possibly London forces, so that the highly porous sock can be handled, stretched and spun into a yarn.

The sock formation process has been studied by numerical simulation and experimental methods<sup>7,8</sup>. The parameter space was studied for a vertical reactor<sup>9</sup> considering the effect of carrier gas and feedstock. Several governing mechanisms for sock formation have been proposed, including thermophoresis or inertial migration<sup>7</sup>, van der Waals attraction<sup>10,11</sup> and electrostatic attraction<sup>12</sup>. In our previous work, a new mechanism for sock formation was also

---

\* Corresponding author. Tel: (513) 556-4132; fax: (513) 556-3390; email: Mark.J.Schulz@uc.edu.

proposed<sup>13</sup>. Lee et al.<sup>14</sup> studied the change of CNT properties, showing that the CNTs have a higher quality (based on Raman Spectroscopy) when a continuous fiber forms. Mikhailchan et al.<sup>15</sup> studied the properties of a CNT aerogel-like assembly, which is produced by depositing a CNT sock on a substrate. The temperature and velocity patterns in a substrate based horizontal reactor were numerically studied by Vahedein<sup>16</sup> using numerical simulation.

Although the sock formation process has been studied by various researchers, there is a lack of understanding of sock properties including sock morphology and even production rate. This knowledge could lead to a better understanding of the sock dynamics and potential routes to improve properties. Moreover understanding sock formation may help produce better CNT yarns. In this work we numerically and experimentally investigate sock dynamics in a multiphysics environment.

## EXPERIMENTAL

A horizontal floating catalyst reactor is employed in this study. Methanol, hexane, ferrocene and thiophene were used as feedstock, which were injected into a 1400 °C reactor along with argon as carrier gas. The detailed parameters were reported in our previous work<sup>13</sup>. Wetting the CNT sock with water shrinks it into CNT thread, which is wound onto a collection bobbin. The CNT sock could also be wound directly on the bobbin for tape production. In this study, the speed of the collection bobbin was adjusted to approximately match the speed of the sock exiting the reactor. The CNT samples were characterized with thermogravimetric analysis (TGA), using a Netzsch STA409 analyzer (samples were heated from room temperature to 900 °C at a rate of 10 °C min<sup>-1</sup> in 30 ml min<sup>-1</sup> in air).

## RESULTS AND DISCUSSION

### Sock dynamics under multiphysics environment

The floating catalyst method for CNT synthesis is a multiphysics process comprising various sub-processes, which include aerosol dynamics, thermal transport, chemical reaction and multiphase flow. The whole process can be separated into three stages based on temperature (Figure 1). After the injection of feedstock into the reactor, the catalyst precursors decompose into iron atoms, which quickly agglomerate to form catalyst particles. In the growth zone, hydrocarbon decomposes and one or more of these decomposition products promotes CNT growth<sup>17</sup>. The CNTs are carried downstream by argon and assemble into a sock under conditions which we will describe below.

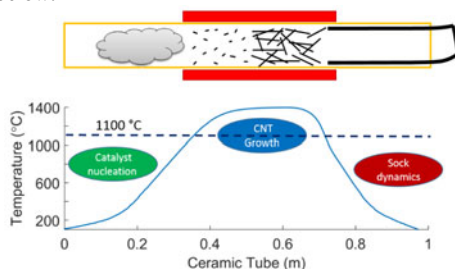


**Figure 1.** Three stages in the floating catalyst synthesis of CNTs.

In order to simplify the analysis, three stages are divided based on the CNT growth temperature. According to our previous results and literature<sup>7,18</sup>, 1100 °C was selected to be the threshold of CNT growth, which is used to define the growth zone. Our previous work<sup>13</sup> shows that a sufficient number of long CNTs would promote the formation of stable socks.

In this work, the sock dynamics at different carrier gas flowrates was studied (Figure 2). The sock morphology changed dramatically when the flowrate was increased from 600 to 2000 sccm. First, the sock is able to continuously exit the reactor at flowrates between 800-1800sccm (the sock formation zone). At a 600sccm flowrate, the CNTs accumulated in the reactor, and curly CNT strands formed without sock formation. At a 2000sccm flowrate, the sock broke and could not maintain any pattern, probably due to the high drag force. Second, the change in the sock pattern in the formation zone (800-1800sccm) is related to CNT-flow field interaction. This is a complex multiphase flow problem including assembly of CNTs into the sock under the influence of heat and flow fields, and two-way interaction between CNTs and the flow field. The previous two stages; (i) catalyst nucleation, and (ii) CNT growth all influence the sock dynamics. In general, the catalyst nucleation process determines the size distribution of the catalyst particles and their spread throughout the growth zone, which affects the number of active catalyst particles growing CNTs. In the CNT growth stage, the residence time correlates with the length of CNTs. Long and a sufficient number of CNTs are essential to the CNTs assembly, and they influence the sock dynamics significantly.

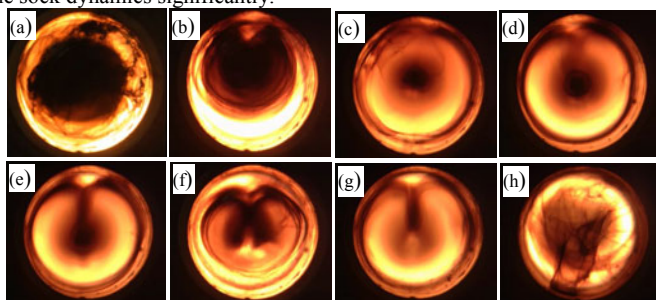


**Figure 2.** Sock dynamics under different carrier gas flowrates: (a) 600 sccm; (b) 800 sccm; (c) 1000 sccm; (d) 1200 sccm; (e) 1400 sccm; (f) 1600 sccm (g) 1800 sccm (h) 2000 sccm. The temperature is 1400 °C, feedstock injection rate is 32 ml/h, and ferrocene 1 wt%.

To understand the sock dynamics, the multiphysics environment was numerically studied using the computational fluid dynamics package FLUENT<sup>TM</sup>. The temperature and velocity along the reactor tube axis were calculated (Figure 3). It could be noted that the temperature profile shifts downstream due to the cold carrier gas flow. This will affect the length and position of the growth zone in the reactor. In Figure 3b, the velocity peak and valley indicates the flow vortex regions. Assuming a straight path along the axis, the catalyst particle residence time has been calculated (Figure 3c). As expected, the residence time reduces from 5.81s to 1.72s when the carrier gas increases from 600 to 2000 SCCM. This may explain the appearance of a thinner sock at the higher flowrate (Figure 2), since the CNTs at higher gas flow are shorter due to a shorter growth time. Eventually at 2000 sccm, the CNTs are too short to entangle with each other and form significant webs. This factor of short CNTs and possible high drag force together lead to the failure to form a sock 2000 SCCM. We have also observed that the CNT properties are

higher at higher temperatures (1400 °C) than at relatively lower temperature (1200 °C). It is believed that higher temperature leads to faster growth and higher quality with less amorphous impurities. This is currently under further study.

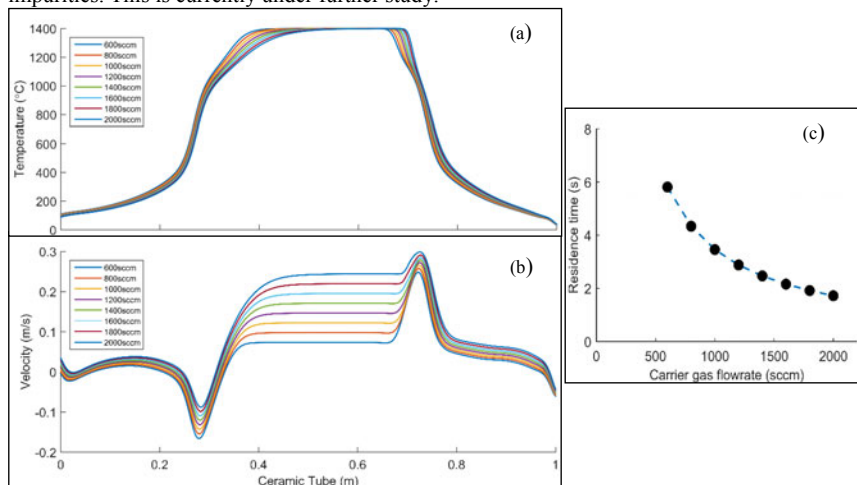


**Figure 3.** Simulation results of the nanotube reactor: (a) Horizontal temperature; (b) velocity; and (c) residence time along tube axis under different gas flowrates.

The vortices around the two ends of growth zone (Figure 3) also influence sock dynamics. More detail of the two vortex in 3D streamline are described in our previous work<sup>13</sup>. As shown in Figure 3, the backflow around the inlet vortex weakens with higher carrier gas flowrate. The backflow around the outlet vortex is suppressed when increasing the carrier gas flowrate. The influence of inlet vortices on the catalyst nucleation is complicated. This vortex will transport small portions of catalyst backward increasing the particle collision time to promote larger catalyst particles. Meanwhile the vortex also increases the chance of catalyst particles sticking on the reactor wall, thus reducing the effective number of catalyst for later CNT growth.

From the above numerical and experimental studies, the complex multiphysics synthesis environment was further revealed. The influence of carrier gas flowrate on all three stages of CNT synthesis was investigated. For production of a stable sock with high quality CNTs, similar simulation and analysis strategies should be considered to control the multiphysics environment.

### **The Sock Production Rate**

To achieve large-scale production of CNT material, it is important to understand the process variables affecting the production rate (g/h). TGA was used to study the amount of iron in the sock (defined as *effective catalyst*, including both unreacted iron and iron nucleating CNTs). It was found that the sock production rate is closely related to the amount of effective iron. As shown in Figure 4, the sock production rate increases with higher content of catalyst precursor (higher injection rate or higher ferrocene concentration), which leads to more catalyst thus more CNTs produced. However the production rate approaches an upper limit. For example the 2 wt% and 1.5 wt% ferrocene samples have a similar production rate around 0.22g/h (Figure 4b).

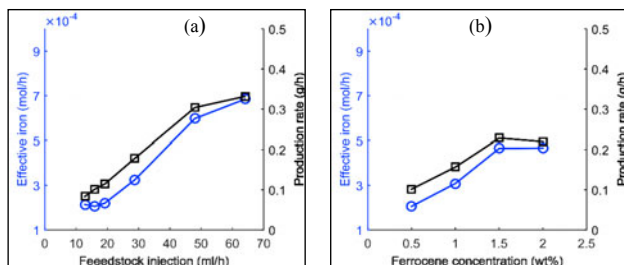


**Figure 4.** Influence of (a) feedstock injection rate; and (b) ferrocene concentration on sock production rate and effective iron.

With the total amount of iron calculated from feedstock injection, the percentage of effective iron ( $Fe_{sock}/Fe_{total}$ ) can be calculated. In most of the cases, the ratio of effective iron was found to be less than 50% as shown in Figure 5. It has also been discovered that when the total amount of iron atoms in the reactor increases, the percentage of effective iron in the sock decreases.

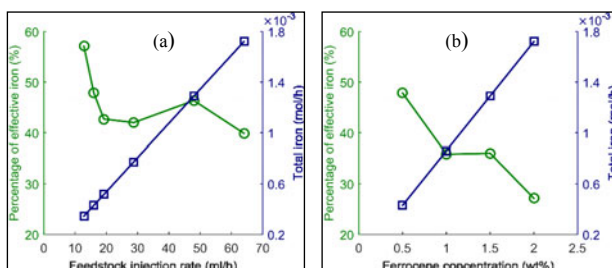


**Figure 5.** Percentage of effective iron (measured by TGA) and total iron (iron added by injecting ferrocene): (a) Influence of feedstock injection rate; (b) Influence of ferrocene concentration.

In order to increase the yield, two synthesis strategies are apparent; (1) increasing the percentage of effective iron; and (2) growing longer CNTs. The low percentage of effective catalyst implies that large amount of Fe is either deposited on the reactor wall or displaced by the carrier gas. When the iron catalyst size is too large, it does not promote CNT growth and leads to a higher chance of being deposited onto the wall or carried out from the reactor. Thus the percentage of effective iron could be optimized by controlling the size of the iron catalyst with smaller catalyst being strongly favored. Growing longer CNT could also increase the yield. One potential method is to control the composition of catalyst particle<sup>19</sup> and grow long CNTs.

## CONCLUSIONS

The CNT sock properties in a floating catalyst reactor has been generally studied numerically and experimentally. The sock formation is a result of two-way interaction between CNTs and the multiphysics environment. Moreover it is closely related with catalyst nucleation and CNT growth. The increasing of gas flow has a diminishing effect on the sock formation

process. Study of sock production rate shows that it is critical to have a high proportion of effective catalyst while increasing the amount of total catalyst in the reactor. Controlling the catalyst size and growing longer CNTs is another potential method to increase the yield.

## ACKNOWLEDGEMENTS

This work was partly supported by the University of Cincinnati Accelerator Program under the Direction of Dr. Dorothy Air, and ONR Award N00014-15-1-2473 under Program Manager Dr. Ignacio Perez. We sincerely thank Dr. David Lashmore from the University of New Hampshire for his valuable discussions.

## REFERENCES

- <sup>1</sup> D. Sun, M.Y. Timmermans, Y. Tian, A.G. Nasibulin, E.I. Kauppinen, S. Kishimoto, T. Mizutani, and Y. Ohno, *Nat. Nanotechnol.* **6**, 156 (2011).
- <sup>2</sup> G. Hou, L. Zhang, V. Ng, Z. Wu, and M. Schulz, *Nano Life* **6**, 1642006 (2016).
- <sup>3</sup> Y. Song, D. Chauhan, G. Hou, X. Wen, M. Kattoura, and C. Ryan, in *ASC 31st Tech. Conf. Williamsbg. VA* (2016).
- <sup>4</sup> N.T. Alvarez, P. Miller, M. Haase, N. Kienzle, L. Zhang, M.J. Schulz, and V. Shanov, *Carbon N. Y.* **86**, 350 (2015).
- <sup>5</sup> S. Zhang, K.K.K. Koziol, I. a Kinloch, and A.H. Windle, *Small* **4**, 1217 (2008).
- <sup>6</sup> Y.-L. Li, I. a Kinloch, and A.H. Windle, *Science* **304**, 276 (2004).
- <sup>7</sup> D. Conroy, A. Moiala, S. Cardoso, A. Windle, and J. Davidson, *Chem. Eng. Sci.* **65**, 2965 (2010).
- <sup>8</sup> K.-H. Lee, S.-H. Lee, J. Park, H.-R. Kim, and J. Lee, *RSC Adv.* 41894 (2015).
- <sup>9</sup> M. Motta, I. Kinloch, A. Moiala, V. Premnath, M. Pick, and A. Windle, *Phys. E Low-Dimensional Syst. Nanostructures* **37**, 40 (2007).
- <sup>10</sup> X.-H. Zhong, Y.-L. Li, J.-M. Feng, Y.-R. Kang, and S.-S. Han, *Nanoscale* **4**, 5614 (2012).
- <sup>11</sup> X.H. Zhong, Y.L. Li, Y.K. Liu, X.H. Qiao, Y. Feng, J. Liang, J. Jin, L. Zhu, F. Hou, and J.Y. Li, *Adv. Mater.* **22**, 692 (2010).
- <sup>12</sup> J. Chaffee, D. Lashmore, D. Lewis, J. Mann, M. Schauer, and B. White, *Nsti Nanotech 2008, Vol 3, Tech. Proc.* **3**, 118 (2008).
- <sup>13</sup> G. Hou, R. Su, A. Wang, V. Ng, W. Li, Y. Song, L. Zhang, M. Sundaram, V. Shanov, D. Mast, D. Lashmore, M. Schulz, and Y. Liu, *Carbon N. Y.* **102**, 513 (2016).
- <sup>14</sup> S.-H. Lee, J. Park, H.-R. Kim, T. Lee, J. Lee, Y.-O. Im, C.-H. Lee, H. Cho, H. Lee, C.-H. Jun, Y.-C. Ahn, I.-B. Lee, and K.-H. Lee, *Carbon N. Y.* **100**, 647 (2016).
- <sup>15</sup> A. Mikhailchan, Z. Fan, T.Q. Tran, P. Liu, V.B.C. Tan, T.-E. Tay, and H.M. Duong, *Carbon N. Y.* **102**, 409 (2016).
- <sup>16</sup> Y.S. Vahedein and M.G. Schrlau, in *13th Int. Conf. Nanochannels, Microchannels, Minichannels* (2015), pp. 0–10.
- <sup>17</sup> E.R. Meshot, D.L. Plata, S. Tawfick, Y. Zhang, E.A. Verploegen, and A.J. Hart, *ACS Nano* **3**, 2477 (2009).
- <sup>18</sup> H.M. Cheng, F. Li, G. Su, H.Y. Pan, L.L. He, X. Sun, and M.S. Dresselhaus, *Appl. Phys. Lett.* **72**, 3282 (1998).
- <sup>19</sup> S.M. Shanov VN, Gorton A, Yun YH, US20080095695 (2014).